Table 6. Other tumors with multiple malignancies (n = 16)

Patient	Age (years)	Gender	FT	Site	CT	RT	MFSP	SPT	Site	CT	RT	MFSP from SPT	TPT	Site	CT	RT	Prognosis	OS
1	62	Female	FS	Thigh	–	–	1	Ad	Uterine	–	–	–	–	–	–	–	DOD	6
2	57	Female	LS (D)	Retroperitoneum	–	40 Gy	29	Ad	Breast	–	–	–	–	–	–	–	DOD	108
3	42	Female	LS (D)	Retroperitoneum	ADR VCR	–	75	Pap	Thyroid	NA	NA	–	–	–	–	–	DOD	78
4	57	Male	LS (M)	Thigh	VCR	–	141	Sq	Larynx	–	60 Gy	–	–	–	–	–	NED	223
5	59	Male	LS (M)	Thigh	–	–	4	Ad	Lung*	–	–	–	–	–	–	–	NED	38
6	61	Male	LS (WD)	Retroperitoneum	–	–	81	Ad	Prostate	SR	62 Gy	–	–	–	–	–	NED	85
7	63	Male	LS (WD)	Retroperitoneum	–	–	8	Ad	Prostate	LA	–	–	–	–	–	–	NED	9
8	70	Female	Ad	Breast	–	–	60	FS	Chest wall	–	–	17	Ad	Stomach	–	–	NED	112
9	60	Male	DLBL	Thyroid	CHOP	–	81	L	Leg	–	–	–	–	–	–	–	NED	117
10	39	Female	Ad	Breast	–	–	60	L	Buttock	CPA, VCR, ADM, DTIC	–	–	–	–	–	–	DOD	212
11	50	Female	Ad	Breast	–	–	105	LS (M)	Thigh	–	50 Gy	–	–	–	–	–	DOD	127
12	64	Male	Ad	Rectum	–	–	50	LS (M)	Leg	–	–	–	–	–	–	–	DOD	61
13	43	Female	Ad	Breast	–	–	102	LS (WD)	Retroperitoneum	–	–	–	–	–	–	–	NED	121
14	63	Female	Ad	Breast	–	–	29	LS (WD)	Retroperitoneum	–	–	–	–	–	–	–	NED	75
15	71	Female	Pap	Thyroid	–	–	2	MPNST	Retroperitoneum	–	–	–	–	–	–	–	NED	15
16	79	Male	TCC	Bladder	–	–	106	Ad	Lung	–	–	12	LS (D)	Retroperitoneum	–	–	DOD	146

FT, first tumor; CT, chemotherapy; RT, radiotherapy; MFSP, malignancy-free survival period (months); SPT, second primary tumor; TPT, third primary tumor; DOD, died of disease; NED, no evidence of disease; OS, overall survival (months); FS, fibrosarcoma; Ad, adenocarcinoma; LS (D), liposarcoma (dedifferentiated); Pap, papillary carcinoma; LS (M), liposarcoma (myxoid); Sq, squamous cell carcinoma; LS (WD), liposarcoma (well differentiated); DLBL, diffuse large B-cell lymphoma; MPNST, malignant peripheral nerve sheath tumor; TCC, transitional cell carcinoma; CHOP, cyclophosphamide, adriamycin, vincristine, prednisolone; ADR, adriamycin; VCR, vincristine; CPA, cyclophosphamide; DTIC, dacarbazine; SR, zoladex; LA, leuplin; NA, not applicable.
*Synchronous tumor.

10 patients (77%). Some investigators consider a pleomorphic MFH to be a high grade tumor that has a substantially high metastatic rate and poor prognosis (17,18). Myxofibrosarcoma is a distinct fibroblastic neoplasm that may recur and has a relatively poor prognosis (19–21). In our study, univariate analysis revealed that no significant association was found between risk of multiple malignancy and survival rate, or familiar history in pleomorphic MFH and myxofibrosarcoma.

A family history of cancer and genetic predisposition to cancer may be associated with a risk of multiple malignancies. A correlation between the incidence of multiple malignancy and familial aggregation has been demonstrated in Li–Fraumeni syndrome (22). Similarly, genetic factors have an impact on the risk of various histological types of SPT (23,24). It was not likely that these factors would profoundly influence the risk related to development of multiple malignancies since there was no significant association between familial history of cancer and the risk of multiple malignancies in our study. Some rare familial syndromes are associated with an excess risk of multiple malignancies. There was a patient with FAP with a germline mutation of the APC gene. This patient developed myxofibrosarcoma of the thigh as a fourth primary tumor after surgical treatment of colon cancers three times.

Despite the fact that the known carcinogenic effects of chemotherapy and radiation therapy are associated with an increased risk of developing SPT (25,26), no interaction was found with having received chemotherapy and radiation therapy according to the results of the multivariate analysis. The lack of agreement between our findings and those of other investigators may be attributable to the small number of patients treated by chemotherapy and radiation therapy: only two patients with second or third primary STS were previously treated by chemotherapy and radiation therapy.

Our results showed that multiple malignancies occurred in 9% of patients with STS, and that the rate of occurrence depended on the histological type. The 5-year survival rate of patients with multiple malignancies according to the histological type of STS was not statistically different from that of the patients without multiple malignancies. Many histological types of multiple malignancies occurred in various organs, suggesting that the whole-body screening to detect other primary malignant neoplasms in addition to local recurrence or distant metastasis should be considered in the management of patients with multiple primary malignancies. Recent prospective studies have highlighted the potential diagnostic role of whole-body [^{18}F]fluorodeoxyglucose positron emission tomography (FDG PET) for evaluation of malignant tumors. FDG PET is an accurate non-invasive test for diagnosis of adult STS and has high sensitivity and intermediate specificity for malignancy. We recommend a whole-body FDG PET scan in the search for a second malignancy in patients with multiple primary malignancies.

In summary, the results of our study confirm the incidence of multiple primary malignancies in adult patients with STS, and the histological type of myxofibrosarcoma was found to be associated with an increased risk of multiple primary malignancy. Physicians should be aware of the increased risk of multiple primary malignancies in patients with myxofibrosarcoma, and whole-body screening to detect other malignant neoplasms is desirable.

References

1. Evans HS, Lewis CM, Robinson D, Bell CMJ, Høller H, Hodgson SV. Incidence of multiple primary cancers in a cohort of women diagnosed with breast cancer in southeast England. *Br J Cancer* 2001;84:435–40.
2. Rubino C, de Vathaire F, Dottorini ME, Hall P, Schvartz C, Couette JE, et al. Second primary malignancies in thyroid cancer patients. *Br J Cancer* 2003;89:1638–44.
3. Leung W, Sandlund JT, Hudson MM, Zhou Y, Hancock ML, Zhu Y, et al. Second malignancy after treatment of childhood non-Hodgkin lymphoma. *Cancer* 2001;92:1959–66.
4. Hasegawa T, Matsuno Y, Niki T, Hirohashi S, Shimoda T, Takayama J, et al. Second primary rhabdomyosarcomas in patients with bilateral retinoblastoma: a clinicopathologic and immunohistochemical study. *Am J Surg Pathol* 1998;22:1351–60.
5. Bokemeyer C, Schmoll HJ. Secondary neoplasms following treatment of malignant germ cell tumors. *J Clin Oncol* 1993;11:1703–9.
6. Hartmann JT, Nichols CR, Droz JP, Horwich A, Gerl A, Fossa SD, et al. The relative risk of second nongerminal malignancies in patients with extragonadal germ cell tumors. *Cancer* 2000;88:2629–35.
7. Heyn R, Haeberlen V, Newton WA, Ragab AH, Raney RB, Tefft M, et al. Second malignant neoplasms in children treated for rhabdomyosarcoma. Intergroup Rhabdomyosarcoma Study Committee. *J Clin Oncol* 1993;11:262–70.
8. Scaradavou A, Heller G, Sklar CA, Ren L, Ghavimi F. Second malignant neoplasms in long-term survivors of childhood rhabdomyosarcoma. *Cancer* 1995;76:1860–7.
9. Pratt CB, Meyer WH, Luo X, Cain AM, Kaste SC, Pappo AS, et al. Second malignant neoplasms occurring in survivors of osteosarcoma. *Cancer* 1997;80:960–5.
10. Aung L, Gorlick RG, Shi W, Thaler H, Shorter NA, Healey JH, et al. Second malignant neoplasms in long-term survivors of osteosarcoma: Memorial Sloan-Kettering Cancer Center Experience. *Cancer* 2002;95:1728–34.
11. Merimsky O, Kollender Y, Issakov J, Bickels J, Flusser G, Gutman M, et al. Multiple primary malignancies in association with soft tissue sarcomas. *Cancer* 2001;91:1363–71.
12. Fletcher CDM, Unni KK, Mertens F, eds. World Health Organization Classification of Tumours. Pathology and Genetics of Tumours of Soft Tissue and Bone. Lyon, France: IARC Press;2002.
13. Hasegawa T, Yamamoto S, Yokoyama R, Umeda T, Matsuno Y, Hirohashi S. Prognostic significance of grading and staging systems using MIB-1 score in adult patients with soft tissue sarcoma of the extremities and trunk. *Cancer* 2002;95:843–51.
14. Kuttesch JF Jr, Wexler LH, Marcus RB, Fairclough D, Weaver-McClure L, White M, et al. Second malignancies after Ewing's sarcoma: radiation dose-dependency of secondary sarcomas. *J Clin Oncol* 1996;14:2818–25.
15. Rich DC, Corpron CA, Smith MB, Black CT, Lally KP, Andrassy RJ. Second malignant neoplasms in children after treatment of soft tissue sarcoma. *J Pediatr Surg* 1997;32:369–372.
16. Green DM, Hyland A, Barcos MP, Reynolds JA, Lee RJ, Hall BC, et al. Second malignant neoplasms after treatment for Hodgkin's disease in childhood or adolescence. *J Clin Oncol* 2000;18:1492–9.
17. Fletcher CD, Gustafson P, Rydholm A, Willen H, Akerman M. Clinicopathologic re-evaluation of 100 malignant fibrous histiocytomas: prognostic relevance of subclassification. *J Clin Oncol* 2001;19:3045–50.
18. Coindre JM, Terrier P, Guillou L, Le Doussal V, Collin F, Ranchere D, et al. Predictive value of grade for metastasis development in the main histologic types of adult soft tissue sarcomas: a study of 1240 patients from the French Federation of Cancer Centers Sarcoma Group. *Cancer* 2001;91:1914–26.
19. Mentzel T, Calonje E, Wadden C, Camplejohn RS, Beham A, Smith MA, et al. Myxofibrosarcoma. Clinicopathologic analysis of 75 cases with emphasis on the low-grade variant. *Am J Surg Pathol* 1996;20:391–405.
20. Weiss SW, Goldblum JR (2001) Fibrosarcoma. In: Enzinger and Weiss's Soft Tissue Tumours, 4th edn. St Louis: Mosby; 2001:423–5.

21. Huang HY, Lal P, Qin J, Brennan MF, Antonescu CR. Low-grade myxofibrosarcoma: a clinicopathologic analysis of 9 cases treated at a single institution with simultaneous assessment of the efficacy of 3-tier and 4-tier grading systems. *Hum Pathol* 2004;35:612–21.
22. Li FP, Fraumeni JF Jr. Prospective study of a family cancer syndrome. *J Am Med Assoc* 1982;247:2692–4.
23. Malkin D, Jolly KW, Barbier N, Look AT, Friend SH, Gebhardt MC, et al. Germline mutations of the p53 tumor-suppressor gene in children and young adults with second malignant neoplasms. *N Engl J Med* 1992;326:1309–15.
24. Kony SJ, de Vathaire F, Chompret A, Shamsaldim A, Grimaud E, Raquin MA, et al. Radiation and genetic factors in the risk of second malignant neoplasms after a first cancer in childhood. *Lancet* 1997; 350:91–5.
25. Chaplain G, Milan C, Sgro C, Carli PM, Bonithon-Kopp C. Increased risk of acute leukemia after adjuvant chemotherapy for breast cancer: a population-based study. *J Clin Oncol* 2000;18:2836–42.
26. Huang J, Mackillop WJ. Increased risk of soft tissue sarcoma after radiotherapy in women with breast carcinoma. *Cancer* 2001;92:172–80.

Mucin-Producing Adenocarcinoma of the Lung

Thin-Section Computed Tomography Findings in 48 Patients and Their Effect on Prognosis

Ukihide Tateishi, MD, PhD, Nestor L. Müller, MD, PhD,§ Takeshi Johkoh, MD, PhD,‖ Arafumi Maeshima, MD, PhD,† Hisao Asamura, MD, PhD,‡ Mitsuo Satake, MD,* Masahiko Kusumoto, MD, PhD,* and Yasuaki Arai, MD, PhD**

Objective: To determine the prognostic value of thin-section computed tomography (CT) findings in patients with mucin-producing adenocarcinoma (MPA) of the lung.

Methods: The study included 48 patients with pathologically proven MPA who had thin-section CT before treatment. The CT findings were correlated with the histopathologic findings and with disease-free survival on follow-up in all patients.

Results: Computed tomography findings identified in patients with MPA of the lung included an air bronchogram (n = 37, 77.1%), areas of ground-glass attenuation (n = 36, 75.0%), areas of air-space consolidation (n = 36, 75.0%), interlobular septal thickening (n = 33, 68.8%), bubble-like lucencies (n = 23, 47.9%), centrilobular nodules (n = 22, 45.8%), and mucus filling of airways (n = 19, 39.6%). Twenty-two (45.8%) of the 48 patients had intrapulmonary metastases. Centrilobular nodules (odds ratio [OR] = 6.7, 95% confidence interval: 1.1–41.4; $P < 0.05$) and mucus filling of airways (OR = 14.4, 95% 95% confidence interval: 2.0–102.7; $P < 0.01$) on thin-section CT were independently associated with an increased likelihood of intrapulmonary metastases. The 5-year disease-free survival rates were 67.9% and 38.4% for patients without and with intrapulmonary metastases, respectively ($P < 0.05$). The presence of centrilobular nodules (relative risk = 10.5, 95% confidence interval: 1.8–59.3; $P < 0.01$) on thin-section CT was an independent predictor of poor prognosis.

Conclusion: Centrilobular nodules on CT are associated with a higher prevalence of intrapulmonary metastases and a poor prognosis in patients with MPA of the lung.

Key Words: mucin-producing tumor, adenocarcinoma, lung, computed tomography

(*J Comput Assist Tomogr* 2005;29:361–368)

Mucin-producing adenocarcinoma (MPA) of the lung is a disorder that includes the histologic category of mucinous bronchioloalveolar carcinoma (BAC) and adenocarcinoma with mixed subtypes according to the World Health Organization classification.[1]

Mucin-producing adenocarcinoma is composed of bronchial, goblet cell–like, tall columnar cells with cytoplasmic mucin and has distinct features, including genetic mutation and antigenic expression by histologic examination.[2–5]

The computed tomography (CT) findings of mucin-producing tumors of the lung have been described.[6–12] Most published data refer to CT findings resulting from mucinous BAC, although 2 studies have included patients with MPA of the lung in their subject groups.[6,7] Characteristic CT findings of mucin-producing tumors of the lung include multiple cysts, cavitation or bubble-like lucencies, an air bronchogram, an interlobular bulging fissure, a CT angiogram sign, and uniform low attenuation of the pulmonary consolidation. To our knowledge, however, there have been no published findings of large series of patients with MPA of the lung who underwent surgical resection, and the prognostic implications of CT findings have not been evaluated.

The aim of the present study was to correlate thin-section CT findings with histopathologic findings and to determine the prognostic value of thin-section CT findings in patients with MPA of the lung.

MATERIALS AND METHODS

A retrospective review of the pathologic records for the period between January 1996 and January 2004 identified 48 treated patients with MPA of the lung. The study population consisted of 24 men and 24 women, with a mean age of 73.1 years (range: 45–85 years). All patients underwent surgical resection, which comprised wedge resection, lobectomy, or pneumonectomy. Twenty-two (45.8%) of these 48 patients also received chemotherapy. Complete resection or sampling of mediastinal or hilar lymph nodes was performed in all

Received for publication November 23, 2004; accepted March 9, 2005.

From the *Division of Diagnostic Radiology, National Cancer Center Hospital and Institute, Tokyo, Japan; †Division of Pathology, National Cancer Center Hospital and Institute, Tokyo, Japan; ‡Division of Thoracic Surgery, National Cancer Center Hospital and Institute, Tokyo, Japan; §Department of Radiology, University of British Colombia and Vancouver Hospital and Health Sciences Centre, Vancouver, British Columbia, Canada; and ‖Department of Medical Physics, Osaka University Graduate School of Medicine, Osaka, Japan.

Reprints: Ukihide Tateishi, Division of Diagnostic Radiology, National Cancer Center Hospital, Tsukiji, Chuo-Ku, 104-0045, Tokyo, Japan (e-mail: utateish@ncc.go.jp).

patients. These included high and low ipsilateral paratracheal, subcarinal, and inferior pulmonary ligament lymph nodes as well as any other suspicious lymph nodes identified at surgery. The tumors were classified according to the current international tumor, node, metastasis (TNM) classification for staging lung cancer after surgery.[13] Of these, 6 tumors (12.5%) were classified as stage Ia, 9 (18.8%) as stage Ib, 8 (16.7%) as stage IIa, 3 (6.3%) as stage IIIa, and 22 (45.8%) as stage IV. Clinical records were available for review in all patients. Clinical histories of cases were also reviewed to identify any underlying medical conditions, the presence or absence of symptoms, and cigarette consumption. Our Institutional Review Board does not require its approval or informed consent for review of patient records and images.

Computed tomography was performed on helical or multidetector scanners (X-Vigor or Aquilion V-detector; Toshiba Medical Systems, Tokyo, Japan). The helical technique in 55 patients consisted of 10.0-mm collimation for individual scans of the entire lung (120 kV[peak], 150 mA) and reconstruction using a standard algorithm. Additional thin-section CT images were obtained in 21 patients using 2.0-mm collimation, a 20-cm field of view, 120 kVp and 200 mA per rotation, 1.0-second gantry rotation, and a high spatial frequency reconstruction algorithm. The remaining 27 patients were evaluated on a multidetector CT scanner using axial 2.0-mm × 4 modes (4 images per gantry rotation), 120 kVp, 200 mA, and 0.5-second scanning time. Thin-section CT images in these 27 patients were obtained using 2.0-mm sections reconstructed at 2.0-mm intervals using a high spatial frequency algorithm and were retrospectively retargeted to each lung with a 20-cm field of view. All patients received iodinated nonionic contrast material intravenously, and the scan delay was set at 40 seconds by autoinjector (Autoenhance A-50 or A-250; Nemoto Kyorindo, Tokyo, Japan). All CT examinations were performed after intravenous administration of contrast. Hard copy images were photographed at window settings for the lung (center, −600 Hounsfield units [HU]; width, 2000 HU) and mediastinum (center, 35 HU; width, 400 HU). The time interval between CT and pathologic diagnosis ranged from 0 to 16 days.

The CT images were assessed in random order by 2 independent observers without reference to the clinical findings. The observers assessed the presence of areas of ground-glass attenuation, air-space consolidation, centrilobular nodules, an air bronchogram, mucus plugging, bubble-like lucencies, bulging of the interlobar fissure, cavitation, traction bronchiectasis or bronchiolectasis, intralobular reticular opacities, interlobular septal thickening, and a CT angiogram. Ground-glass attenuation was defined as an area of hazy increased parenchymal attenuation without obscuration of the underlying vascular markings. Areas of air-space consolidation were considered present when the opacity obscured the underlying vessels. Mucus plugging was defined as tubular attenuation structures resulting from mucus filling of airways. The shape of mucus plugging depends on the branching pattern of involved airways. Bubble-like lucencies were considered present when there was enlargement of multiple cystic air spaces measuring 5 mm or less in diameter within the lesion surrounded by a wall of variable thickness.[14] Bulging of an interlobar fissure was considered to result from expansion of the lobe by the lesion.[15] Cavitation included a circumscribed enlarged air space with a wall of variable thickness.[16,17] Traction bronchiectasis or bronchiolectasis was defined as irregular bronchial dilatation within areas with a parenchymal abnormality. A CT angiogram was considered to have occurred when the enhanced pulmonary vessels could be clearly identified within a lesion of low attenuation relative to the chest wall musculature.[18] The presence of lymphadenopathy and pleural effusions was also noted. Lymphadenopathy was considered present when the short-axis diameter of the nodes was greater than 10 mm. The anatomic distribution was noted to be central if there was a predominance of abnormalities in the inner two thirds of the lung and peripheral if there was a predominance of abnormalities in the outer third of the lung. After initial independent evaluation, the 2 observers reviewed all cases in which they had a discrepant interpretation and reached a final decision by means of consensus.

Surgical specimens were fixed with inflation by transpleural and transbronchial infusion of formalin. The specimens were sectioned transversely in the same plane as that of the CT. All pathologic specimens were stained with hematoxylin-eosin. The presence of mucus retention was assessed by morphologic examination with a histochemical technique using periodic acid–Schiff reagent. The internal characteristics of the tumors seen on thin-section CT were compared with those seen at pathologic examination of the specimens.

Surgical specimens were evaluated by an expert lung pathologist for histologic diagnosis, presence of intrapulmonary metastasis, thickened bronchi or bronchioles, and mucus retention. We defined MPA to indicate classic "diffuse bronchioloalveolar carcinoma" that simulates lobar pneumonia at presentation. Tumor cells of MPA were composed of bronchial, goblet cell–like, tall columnar cells with cytoplasmic mucin. Correlation between the CT and histologic findings was made by consensus between the radiologist, surgeon, and pathologist.

All patients were regularly followed up in our institute. Follow-up CT images were available for all patients. Disease-free survival was calculated from the date of the operation to the date of intrapulmonary metastasis or last contact with the patient. The mean follow-up after surgery was 30.9 months.

Univariate analysis of the thin-section CT findings was performed using the χ^2 test and Fisher exact test. The relation of thin-section CT findings and the presence or absence of intrapulmonary metastasis was tested for independent predictors using multiple logistic regression analysis, which determined the odds ratio (OR) after adjusting for the other variables examined. Interobserver variation for the CT findings was quantified as the weighted κ-coefficient of agreement. A κ-value greater than 0 was considered to indicate a positive correlation, a κ-value of 0–0.20 indicated poor agreement, a κ-value of 0.21–0.40 indicated fair agreement, a κ-value of 0.41–0.60 indicated moderate agreement, a κ-value of 0.61–0.80 indicated good agreement, and a κ-value of 0.81–1.00 indicated excellent agreement. Survival curves were estimated using the Kaplan-Meier method. The univariate influence of thin-section CT findings on survival was analyzed by means of

the log-rank test. The Cox proportional hazard model was applied to all covariates that had shown statistical significance ($P < 0.05$) at the univariate analysis. The Wald test was used in a backward stepwise selection procedure to identify parameters with significant independent predictive value and to estimate the relative risk (RR) and 95% confidence interval. All analyses were performed using SPSS statistical software (version 11.0, SPSS, Chicago, IL).

RESULTS

Patient Characteristics

The clinical characteristics and outcomes of all patients with MPA of the lung are summarized in Table 1. Twenty-two (45.8%) of the 48 patients had intrapulmonary metastases. The age at presentation was significantly higher in patients with intrapulmonary metastases than in those without intrapulmonary metastases. A statistically significant difference was noted in gender as well as in the proportion of smokers between the patients with and without intrapulmonary metastases. Cigarette consumption was not statistically associated with the presence or absence of intrapulmonary metastases, however. The patients with intrapulmonary metastases were more likely to have a large tumor size than those without intrapulmonary metastases.

TABLE 1. Clinical Characteristics and Outcomes of the Study Population

	Intrapulmonary Metastasis (−)	Intrapulmonary Metastasis (+)	*P*
No. patients	26	22	
Age (mean/SD, y)	70.0/11.8	76.8/8.1	<0.05†
Age range (y)	45–83	60–85	
Gender			
Male	9	15	<0.05‡
Female	17	7	
Smoker	5	16	<0.0001‡
Nonsmoker	21	6	
Cigarette consumption (pack years/SD)	8.3/3.6	10.9/3.8	0.63†
Tumor size (cm)			
Mean/SD	4.8/2.9	11.5/4.3	<0.0001†
Range	2.1–13.0	5.6–17.5	
Treatment			
Wedge resection	4	0	
Lobectomy*	22	20	
Pneumonectomy*	0	2	
Follow-up duration after initial diagnosis (mo)			<0.0001†
Median	39.0	17.5	
Mean/SD	41.0/16.8	19.0/9.1	
Range	14–75	4–38	
Mortality (%)	7.7	86.4	<0.0001‡

*Complete resection or sampling of mediastinal and hilar lymph nodes was also performed. Patients with intrapulmonary metastasis who underwent a lobectomy or pneumonectomy also received chemotherapy.

Statistical comparisons were performed between the patients with and without intrapulmonary metastasis using the 2-tailed paired *t* test† and χ^2 test‡.

TABLE 2. Thin-Section CT Findings of Patients With and Without Intrapulmonary Metastasis

CT Findings	Metastasis (−) (n = 26)	Metastasis (+) (n = 22)	*P*
Air bronchogram	81.8	86.4	0.16
Areas of ground-glass attenuation	65.4	86.4	0.09
Areas of air-space consolidation	61.5	90.9	<0.05
Bubble-like lucencies*	46.2	50.0	0.79
Interlobular septal thickening	53.1	27.3	0.89
Centrilobular nodules	15.4	81.8	<0.0001
Mucus filling of airways	7.7	65.4	<0.0001
Bulging of interlobar fissure*	23.1	36.4	0.31
Cavitation	23.1	4.5	0.07
Traction bronchiectasis or bronchiolectasis	26.9	18.1	0.47
Intralobular reticular opacities*	73.1	63.6	0.48

Data are presented as percentages. Differences between 2 groups of intrapulmonary metastasis are compared by the χ^2 test* and Fisher exact probability test.

CT Features

There was good interobserver agreement for the analysis of the thin-section CT findings (weighted κ-value: 0.68–0.74). The CT findings are summarized in Table 2. The CT findings identified frequently in MPA of the lung on univariate analysis included an air bronchogram (n = 37, 77.1%; Fig 1), areas of ground-glass attenuation (n = 36, 75.0%; see Fig 1; Fig 2), areas

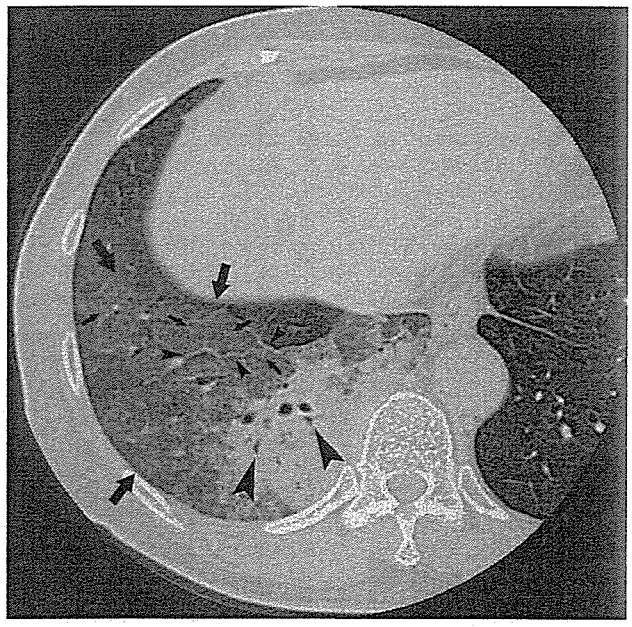

FIGURE 1. Mucin-producing adenocarcinoma of the lung in an 80-year-old woman. A computed tomography image shows a poorly demarcated mass with adjacent areas of ground-glass attenuation (large arrows). Also noted is the presence of an air bronchogram (large arrowheads), interlobular septal thickening (small arrowheads), and intralobular reticular opacities (small arrows).

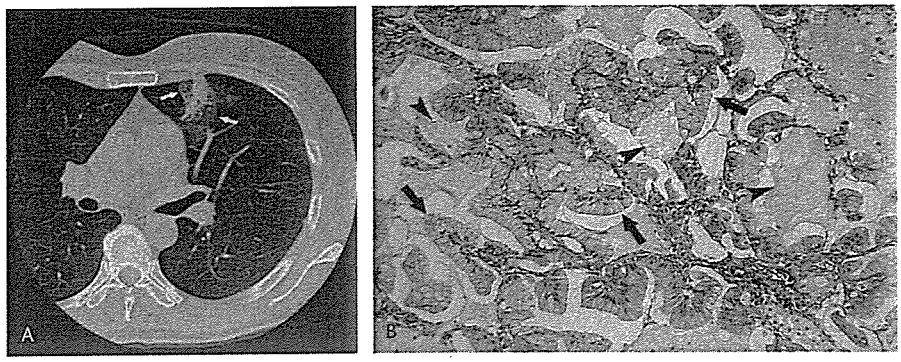

FIGURE 2. Mucin-producing adenocarcinoma of the lung in a 67-year-old woman. A, Thin-section computed tomography image demonstrates areas of ground-glass attenuation (white arrows). B, Pathologic specimen reveals replacement growth of tumor cells (arrows) and the surrounding mucus retention (arrowheads).

of air-space consolidation (n = 36, 75.0%; see Fig.1; Fig 3), and interlobular septal thickening (n = 33, 68.8%; see Fig 1).

Less common CT findings included bubble-like lucencies (n = 23; Fig 5), intralobular reticular opacities (n = 23; see Fig 1), centrilobular nodules (n = 22; Fig 3), mucus plugging (n = 19; Fig 4), bulging of interlobar fissure (n = 14), traction bronchiectasis or bronchiolectasis (n = 11), cavitation (n = 7; Fig 7), and a CT angiogram (n = 4). Mucus plugging, when present, was always superimposed on areas of air-space consolidation or ground-glass attenuation. Pleural effusion was also noted in 2 patients.

Correlation Between Intrapulmonary Metastases and CT Findings

Univariate analysis demonstrated that areas of air-space consolidation, centrilobular nodules, and mucus plugging were significantly associated with an increased likelihood of intrapulmonary metastases (see Table 2). There was no statistically significant difference in the frequency of areas of ground-glass attenuation, air bronchogram, bubble-like lucencies, bulging of the interlobar fissure, cavitation, traction bronchiectasis or bronchiolectasis, interlobular septal thickening, and intralobular reticular opacities among patients with and without intrapulmonary metastases. Multiple logistic regression analysis demonstrated that the thin-section CT findings independently associated with an increased likelihood of intrapulmonary metastases were centrilobular nodules (OR = 6.7; $P < 0.05$) and mucus plugging (OR = 14.4; $P < 0.05$; Table 3).

Correlation Between CT and Histopathologic Findings

Tumors with the focal type of lung involvement were well-demarcated nodular tumors growing along alveolar walls and associated with marked mucin production. Tumors with intrapulmonary metastases were multifocal and had poorly defined margins. Areas of ground-glass attenuation on thin-section CT correlated with the replacement growth of tumor cells or mucus (see Fig 2). Mucus resulted in filling of alveolar spaces in all patients. Areas of air-space consolidation corresponded to a mixture of tumor cells, mucus, and decreased air content in alveolar spaces. Bubble-like lucencies on thin-section CT corresponded histologically to a mixture of mucus, goblet type tumor cells, thickened and dilated bronchi or bronchioles, and small amounts of air in alveolar spaces. Thickened and dilated bronchi or bronchioles, which were often accompanied by localized scarring, focal alveolar collapse, and organized pneumonia, were found mainly in the distal periphery of the tumor. Intralobular reticular opacities correlated with the presence of alveoli filled with mucus and the preserved alveolar septa or underlying parenchyma. Interlobular septal thickening on thin-section CT corresponded to infiltration of the interstitium by inflammatory cells or septal edema. The sensitivity and specificity of centrilobular nodules in detecting intrapulmonary metastases were 81.8% (18 of 22 patients) and 84.6% (22 of 26 patients), respectively. Metastatic lesions often contained an aerated bronchiole. In 4 patients (8.3%), the intrapulmonary metastases were minute and were only identified with difficulty on

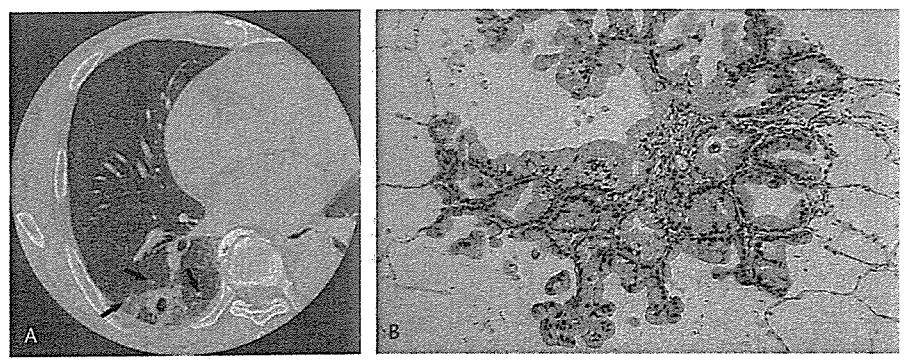

FIGURE 3. Mucin-producing adenocarcinoma of the lung in a 55-year-old man. A, Thin-section computed tomography image shows the tumor with surrounding centrilobular nodules (arrows). B, Microscopic observation reveals intrapulmonary metastasis containing abundant tumor cells and mucin.

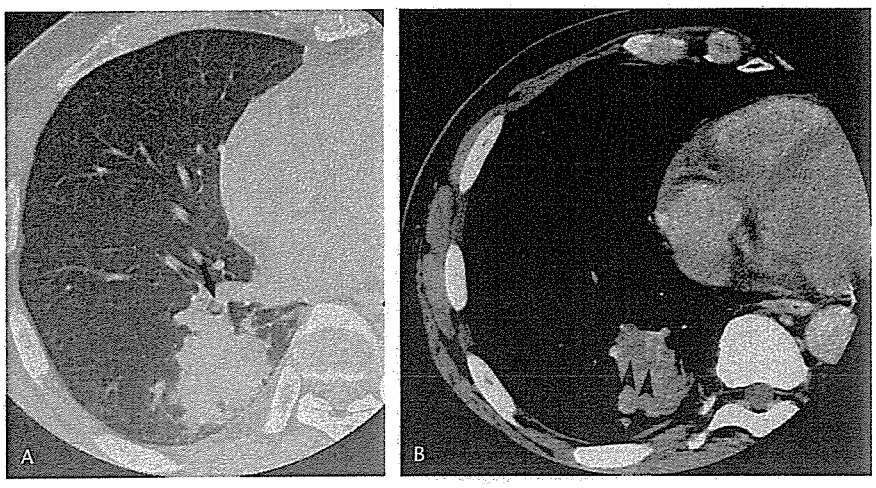

FIGURE 4. Mucin-producing adenocarcinoma of the lung in an 84-year-old man. A, Thin-section computed tomography image shows a poorly demarcated mass with mucus plugging (arrow). B, Thin-section CT image obtained 25 mm below the level of A shows tubular low attenuation of mucus plugging (arrowheads) in the lumen of a dilated peripheral bronchus in the mediastinal window setting.

the corresponding CT images. The CT halo sign identified on thin-section CT corresponded to a tumor component with a bronchioalveolar or papillary growth pattern and mucus layer excreted by surrounding tumor cells.

Clinical Outcome and Prognostic Analysis

Follow-up duration and mortality are summarized in Table 1. A statistically significant difference was found in follow-up duration after an initial diagnosis between the patients with and without intrapulmonary metastases ($P < 0.05$). Twenty-six (54.2%) of 48 patients had no evidence of recurrent disease. Twenty-four (92.3%) of 26 patients without intrapulmonary metastases and 3 (38.5%) of 22 patients with intrapulmonary metastases were alive. There was a significantly higher mortality rate of the patients with intrapulmonary metastases compared with the patients without metastases (see Table 1).

Univariate analysis demonstrated that areas of centrilobular nodules, mucus plugging, interlobular septal thickening, and a CT angiogram were significant predictors of poor prognosis in patients with MPA of the lung (Table 4). No significant predictors of poor prognosis were identified in thin-section CT findings, which included areas of ground-glass attenuation, areas of air-space consolidation, an air bronchogram, bubble-like lucencies, bulging of the interlobar fissure, cavitation, traction bronchiectasis or bronchiolectasis, and intralobular reticular opacities. The 5-year disease-free survival rates for those patients not having and having intrapulmonary metastases were 67.9% and 38.4%, respectively ($P < 0.05$; Fig 6). Age, gender, smoking history, and cigarette consumption had no significant prognostic value. Cox proportional hazard analysis demonstrated that the presence of centrilobular nodules (RR = 10.5; $P < 0.01$) on thin-section CT was an independent predictor of poor prognosis (Figs 7,8; Table 5).

DISCUSSION

In this study, we examined the correlation between thin-section CT findings and histopathologic findings to determine the prognostic value of thin-section CT findings in patients with MPA of the lung. We found that the presence of centrilobular nodules and mucus plugging on thin-section CT was associated with an increased likelihood of intrapulmonary metastases and that the presence of centrilobular nodules was strongly predictive of a poor prognosis.

Several groups of investigators have demonstrated that MPA of the lung has distinct genetic and immunohistochemical features.[2–5] Immunohistochemical staining, including lysozyme and epithelial mucinous glycoprotein, has revealed

FIGURE 5. Mucin-producing adenocarcinoma of the lung in a 76-year-old man. Thin-section computed tomography image shows areas of air-space consolidation with bubble-like lucencies (arrows).

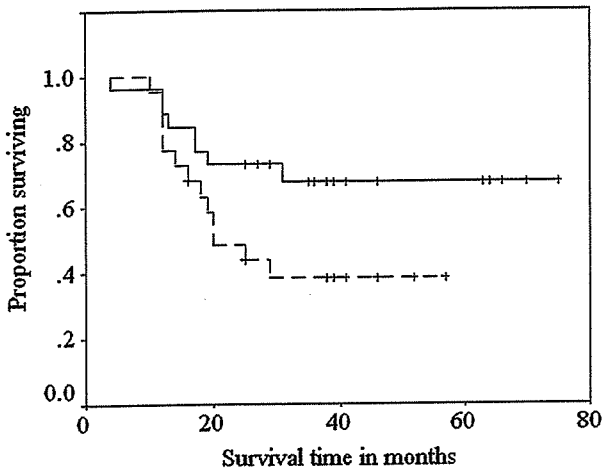

FIGURE 6. Kaplan-Meier survival curves for patients with mucin-producing adenocarcinoma of the lung grouped by the presence (n = 22, dashed line) and absence (n = 26, solid line; $P < 0.05$) of intrapulmonary metastases.

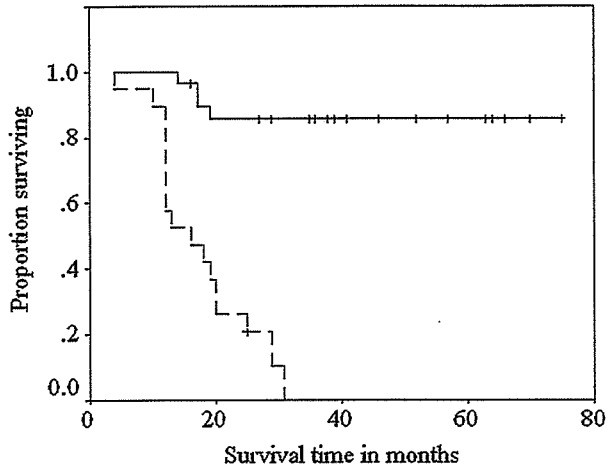

FIGURE 8. Kaplan-Meier survival curves for patients with mucin-producing adenocarcinoma of the lung grouped by the presence (n = 19, dashed line) and absence (n = 29, solid line; $P < 0.0001$) of mucus plugging on thin-section computed tomography.

that MPA of the lung has a specific pattern of mucin gene expression different from those of other types of lung adenocarcinoma.[4] Mucin-producing adenocarcinoma of the lung also has a greater prevalence of intrapulmonary metastases than other subtypes of lung adenocarcinoma.[2–5] These characteristics are at least partly responsible for the poor prognosis of MPA of the lung.

Mucin-producing adenocarcinoma of the lung exhibited a variety of CT features in our study. Characteristic CT features in patients with MPA of the lung are an air bronchogram, areas of ground-glass attenuation, areas of air-space consolidation, and interlobular septal thickening. An air bronchogram, likely caused by parenchymal invasion by tumor cells and mucus secretion, was present to some degree in 37 study patients.

Areas of ground-glass attenuation were present in 36 (75.0%) of our 48 patients with MPA of the lung and correlated pathologically with lepidic growth of the tumor along alveolar septa (replacement growth) or with the presence of mucus. These findings are similar to those reported for mucinous BAC in previous studies,[8–12] which also showed that areas of ground-glass attenuation can progress to areas of air-space consolidation on sequential CT scans. Multivariate analysis showed no association between ground-glass attenuation and the presence or absence of intrapulmonary metastases or prognosis, however.

Areas of air-space consolidation identified in 75.0% of our cases correlated pathologically with a mixture of tumor cells, mucus, and decreased air content in alveolar spaces. Our results suggest that areas of air-space consolidation can result from dense growth of tumor cells or accumulation of mucus within the lesion. In the current study, a significant difference was found in occurrence of areas of air-space consolidation among the patients with and without intrapulmonary metastases. These results are in keeping with those for mucinous BAC in previously published studies.[8–12] Multivariate analysis

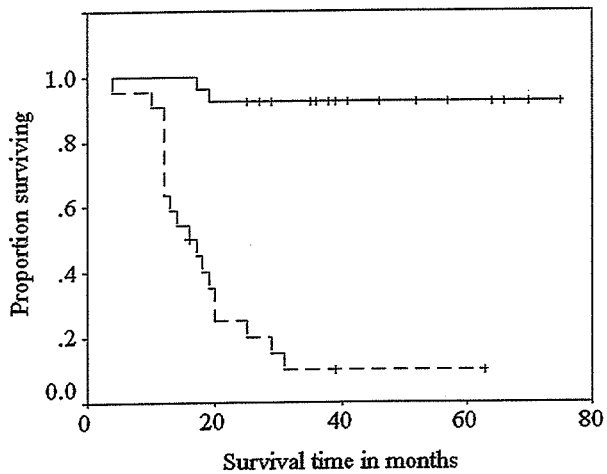

FIGURE 7. Kaplan-Meier survival curves for patients with mucin-producing adenocarcinoma of the lung grouped by the presence (n = 22, dashed line) and absence (n = 26, solid line; $P < 0.0001$) of centrilobular nodules on thin-section computed tomography.

TABLE 3. Multiple Logistic Regression Analysis of Thin-Section CT Findings Associated With Intrapulmonary Metastasis

CT Findings	OR	95% CI	P
Presence of centrilobular nodules (vs. absence)	6.7	1.1–41.4	<0.05
Presence of mucus filling of airways (vs. absence)	14.4	2.0–102.7	<0.01

OR associated with intrapulmonary metastasis is estimated for thin-section CT findings.
95% CI indicates 95% confidence interval.

TABLE 4. Univariate Analysis of Thin-Section CT Findings on 5-Year Disease-Free Survival in Patients With MPA of the Lung

CT Findings	5-Year DFS Rate of Patients With Absent CT Finding (%)	n (%)	5-Year DFS Rate of Patients With Present CT Finding (%)	n (%)	Log Rank *P*
Air bronchogram	72.7	11 (22.9)	49.4	37 (77.1)	0.33
Area of ground-glass attenuation	66.7	12 (25.0)	49.9	36 (75.0)	0.45
Areas of air-space consolidation	83.3	12 (25.0)	44.9	36 (75.0)	0.06
Bubble-like lucencies	46.7	25 (52.1)	64.5	23 (47.9)	0.31
Interlobular septal thickening	61.9	15 (31.3)	38.1	33 (68.8)	<0.05
Centrilobular nodules	92.3	36 (75.0)	10.0	12 (25.0)	<0.0001
Mucus filing of airways	85.8	29 (60.4)	0.0	19 (39.6)	<0.0001
Bulging of interlobar fissure	59.8	34 (70.8)	42.9	14 (29.2)	0.23
Cavitation	53.4	41 (85.4)	55.6	7 (14.6)	0.43
Traction bronchiectasis or bronchiolectasis	54.4	37 (77.1)	54.6	11 (22.9)	0.91
Intralobular reticular opacities	57.6	43 (89.6)	40.0	5 (10.4)	0.80

Patients were stratified by the presence or absence of each thin-section CT finding on survival.
DFS indicates disease-free survival; MPA, mucin-producing adenocarcinoma.

showed that areas of air-space consolidation are not an independent predictor of intrapulmonary metastasis and prognosis, however.

Bubble-like lucencies on thin-section CT are characterized by the presence of small focal areas of air attenuation within the lesion. The presence of bubble-like lucencies in our study was similar to that reported for mucinous BAC in another study.[11] In our study, bubble-like lucencies on thin-section CT corresponded histologically to a mixture of mucus, tumor cells, thickened bronchi or bronchioles, and small amounts of air in alveolar spaces. Although bubble-like lucencies were seen in 47.9% of our cases, this finding was not a predictor of intrapulmonary metastasis or survival.

Centrilobular nodules were present in 45.8% of our cases. This prevalence is in agreement with that reported for mucinous BAC in previous studies.[8–12] In our study, 81.8% of patients with centrilobular nodules had intrapulmonary metastases. Multivariate analysis demonstrated that centrilobular nodules were an independent predictor of poor prognosis. These results may reflect multifocal abnormalities of mucus lining and true metastases on CT.

Mucus plugging was identified in 39.6% of our cases on thin-section CT. This finding had a significant association with the presence of intrapulmonary metastases and survival in univariate analysis. Multivariate analysis demonstrated that mucus plugging was not an independent predictor of poor prognosis, however. Mucus plugging is considered to be more nonspecific compared with centrilobular nodules, which can manifest the presence of true metastases on thin-section CT.

The limitation of our study is that bias was probably introduced by including 45.8% of patients who had intrapulmonary metastases and underwent surgical treatment and chemotherapy. These patients had the smallest rate of 5-year disease-free survival, leading to possible selection bias that would tend to overestimate the prevalence of intrapulmonary metastases.

In conclusion, the presence of centrilobular nodules and mucus plugging on thin-section CT is associated with a greater likelihood of intrapulmonary metastases. The presence of centrilobular nodules is also a predictor of a poor prognosis in patients with MPA of the lung.

TABLE 5. Cox Proportional Hazard Analysis of Thin-Section CT Findings on 5-Year Disease-Free Survival in Patients With MPA of the Lung

CT Findings	RR	95% CI	*P*
Presence of centrilobular nodules (vs. absence)	10.5	1.9–59.3	<0.01

RR associated with patient death is estimated for CT findings.
95% CI indicates 95% confidence interval; MPA, mucin-producing adenocarcinoma.

REFERENCES

1. Travis WD, Colby TV, Corrin B, et al. Histological typing of lung and pleural tumors In: *International Histological Classification of Tumors*. 3rd ed. Geneva: World Health Organization; 1999.
2. Gemma A, Noguchi M, Hirohashi S, et al. Clinicopathologic and immunohistochemical characteristics of goblet cell type adenocarcinoma of the lung. *Acta Pathol Jpn*. 1991;41:737–743.
3. Tsuchiya E, Furuta R, Wada N, et al. High K-ras mutation rates in goblet-cell-type adenocarcinomas of the lungs. *J Cancer Res Clin Oncol*. 1995; 121:577–581.

4. Maeshima A, Miyagi A, Hirai T, et al. Mucin-producing adenocarcinoma of the lung, with special reference to goblet cell type adenocarcinoma: immunohistochemical observation and Ki-ras gene mutation. *Pathol Int.* 1997;47:454–460.
5. Maeshima A, Sakamoto M, Hirohashi S. Mixed mucinous-type and non-mucinous-type adenocarcinoma of the lung: immunohistochemical examination and K-ras gene mutation. *Virchows Arch.* 2002;440:598–603.
6. Gaeta M, Vinci S, Minutoli F, et al. CT and MRI findings of mucin-containing tumors and pseudotumors of the thorax: pictorial review. *Eur Radiol.* 2002;12:181–189.
7. Miyake H, Matsumoto A, Terada A, et al. Mucin-producing tumor of the lung: CT findings. *J Thorac Imaging.* 1995;10:96–98.
8. Kuhlman JE, Fishman EK, Kuhajda FP, et al. Solitary bronchioloalveolar carcinoma: CT criteria. *Radiology.* 1988;167:379–382.
9. Aquino SL, Chiles C, Halford P. Distinction of consolidative bronchioloalveolar carcinoma from pneumonia: do CT criteria work? *AJR Am J Roentgenol.* 1998;171:359–363.
10. Akira M, Atagi S, Kawahara M, et al. High-resolution CT findings of diffuse bronchioloalveolar carcinoma in 38 patients. *AJR Am J Roentgenol.* 1999;173:1623–1629.
11. Mihara N, Ichikado K, Johkoh T, et al. The subtypes of localized bronchioloalveolar carcinoma: CT-pathologic correlations in 18 cases. *AJR Am J Roentgenol.* 1999;173:75–79.
12. Jung JI, Kim H, Park SH, et al. CT differentiation of pneumonic-type bronchioloalveolar cell carcinoma and infectious pneumonia. *Br J Radiol.* 2001;74:490–494.
13. Lababede O, Meziane MA, Rice TW. TNM staging of lung cancer: a quick reference chart. *Chest.* 1999;115:233–235.
14. Adler B, Padley S, Miller RR, et al. High-resolution CT of bronchioloalveolar carcinoma. *AJR Am J Roentgenol.* 1992;159:275–277.
15. Barnes DJ, Naraqi S, Igo JD. The role of percutaneous lung aspiration in the bacteriological diagnosis of pneumonia in adults. *Aust NZ J Med.* 1988;18:754–757.
16. Weisbrod GL, Towers MJ, Chamberlain DW, et al. Thin-walled cystic lesions in bronchioalveolar carcinoma. *Radiology.* 1992;185:401–405.
17. Gaeta M, Caruso R, Blandino A, et al. Radiolucencies and cavitation in bronchioloalveolar carcinoma: CT-pathologic correlation. *Eur Radiol.* 1999;9:55–59.
18. Im JG, Han MC, Yu EJ, et al. Lobar bronchioloalveolar carcinoma: "angiogram sign" on CT scans. *Radiology.* 1990;176:749–753.

特集

癌緩和医療

癌緩和医療における Interventional radiology (IVR)

荒井保明[*1]　佐竹光夫[*1]　稲葉吉隆[*2]　新槇　剛[*3]
松枝　清[*4]

Interventional Radiology for Palliative Care: Arai Y[*1], Satake M[*1], Inaba Y[*2], Aramaki T[*3] and Matsueda K[*4] ([*1]Dept of Diagnostic Radiology, National Cancer Center, [*2]Dept of Diagnostic Radiology, Aichi Cancer Center, [*3]Dept of Diagnostic Imaging, Shizuoka Cancer Center, [*4]Dept of Diagnostic Imaging, Cancer Foundation, Ariake Hospital)

Interventional radiology is image-guided percutaneous treatment and it can revise intra-physical abnormal structural or physiological conditions without major invasion. Thus, interventional radiology has much potential for better management of various symptoms caused by cancer progression, such as ductal stenosis, fluid collection, unremoval tubes, etc. Additionally, using techniques of interventional radiology, many kinds of procedure for palliative care can be done more safety, easier and less invasive. Medical stuffs who are concerned in palliative care should have knowledge about interventional radiology and make full use it for their daily works.

Key words: Interventional radiology, Palliative care, QOL, Metallic stent, Drainage
Jpn J Cancer Clin **51**(3): 213～220, 2005

はじめに

インターベンショナル・ラジオロジー（Interventional radiology）は従来画像診断に用いられていた装置や器具を用いて，画像誘導下に外科的に身体を開けることなく治療を行うものである．Interventional radiology の語源は Margulis が1967年に提唱した Interventional Diagnostic Radiology[1]に由来しており，現在のような体系づけと Interventional radiology という言葉の紹介は1976年に Wallace が Cancer に載せた総説[2]に始まる．日本語訳として普及したものがないため，インターベンショナル・ラジオロジーあるいは略して IVR, IR と呼称される場合が多い（本稿では以下 IVR と略す）．わが国では1980年代より普及し，その後画像診断機器ならびに器材の急速な進歩に伴い広い範囲で活用されるに至っている．その特長は何といっても外科治療に比べ侵襲の少ない点であり，このため QOL が重視されるがん治療での活用範囲は広く，緩和医療（active palliation）において重要な役割を担うに至っている．本稿では癌緩和医療における IVR について述べる．

*1 国立がんセンター中央病院放射線診断部
*2 愛知県がんセンター放射線診断部
*3 静岡県立静岡がんセンター画像診断科
*4 癌研究会有明病院画像診断部

1. 癌緩和医療における IVR の原理

IVR における画像誘導下での病巣への到達は，カテーテルを用いて血管をはじめとする既存の管腔臓器を介する場合と，針を用いて穿刺により直線的に到達する場合とに大別される．到達した病巣部で行う処置は，液体・気体の注入，吸引あるいは移動，器具を用いた管腔臓器の閉塞，拡張，凝固，凍結などであり，数多い IVR も基本的にはこれらの手技の組み合わせによって行われ

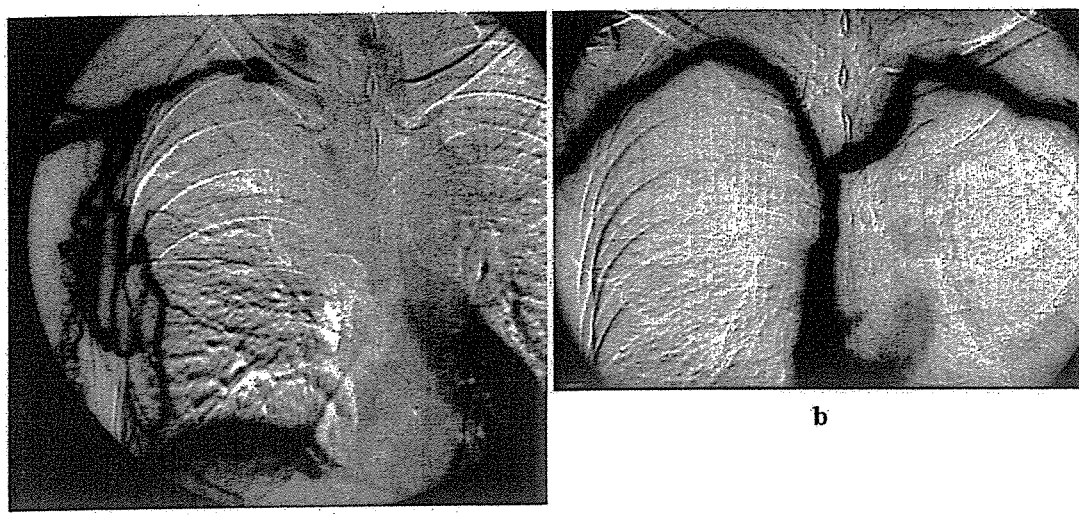

a　b

図1　上大静脈症候群に対するステント留置
a：肺がんにより右鎖骨下静脈-上大静脈は閉塞し，右上肢から注入された造影剤は右房に戻ることなく，胸壁の静脈に逆流している．
b：右鎖骨下静脈-上大静脈へのステント留置により，左右上肢から注入された造影剤は速やかに右房に還流している．

るものである．癌緩和医療におけるIVRはこれらの手技を用いて，癌の進展により身体の正常構築や生理的状態が破綻して生じた「異常な状態」をより正常に近い，より生理的な状態に戻すことにより，その「異常な状態」に起因する症状を軽減，消失させようとするものである．このため，症状の原因自体に対する治療という点で，他の症状を対象とする治療とは原理的に大きく異なっている．

2.　管腔臓器の狭窄・閉塞に対する治療

身体は血管，消化管，気管，胆管など基本的に管腔臓器の集合体であり，このため，癌の進展によりこれらの管腔臓器が狭窄・閉塞することにより種々の症状が発現する．IVRによる治療はこれら管腔臓器の狭窄・閉塞をメタリック・ステントの留置により解除するもので，管腔臓器の生理的機能を回復することにより症状を軽減するものである．現在対象とされる管腔臓器は，上下大静脈，気道，食道を主とする上部消化管，直腸に近い下部消化管，胆道などである．

1）大静脈の狭窄に対する治療（図1）

肺癌，乳癌などによる上大静脈症候群，肝腫瘍の増大などにより生じた下大静脈の狭窄に起因する腹水・下肢の浮腫などが対象となる．通常は局所麻酔下に大腿静脈から挿入したカテーテルを介して，狭窄部にステントを留置する（図1, 2）．119症例を対象とした厚生省がん研究助成金（荒井班）[3~7]による共同研究では，技術的成功率100%，重篤な合併症はなく，明らかな臨床症状の改善が84%で得られている．本治療は大静脈系の狭窄・閉塞に対する唯一の原因除去療法であり，その安全性，有効性の点からも試みるべき治療法といえる．

2）気道の狭窄に対する治療（図2）

メタリック・ステントの挿入により気道狭窄に伴う呼吸困難を改善するものであり，狭窄部が気管，左右主気管支レベルで末梢肺の機能が維持されている場合が対象となる．89例を対象に行われた厚生省がん研究助成金（荒井班）による共同研究では，技術的成功率100%，重篤な合併症はなく，臨床症状の改善が83%にみられている．うち60%の症例ではHugh-Jones分類で2段階以上の改善が得られ，治療前人工呼吸器が使用されていた7例全例が呼吸器管理から離脱，また，術前酸素吸入を要した29例中17例が酸素

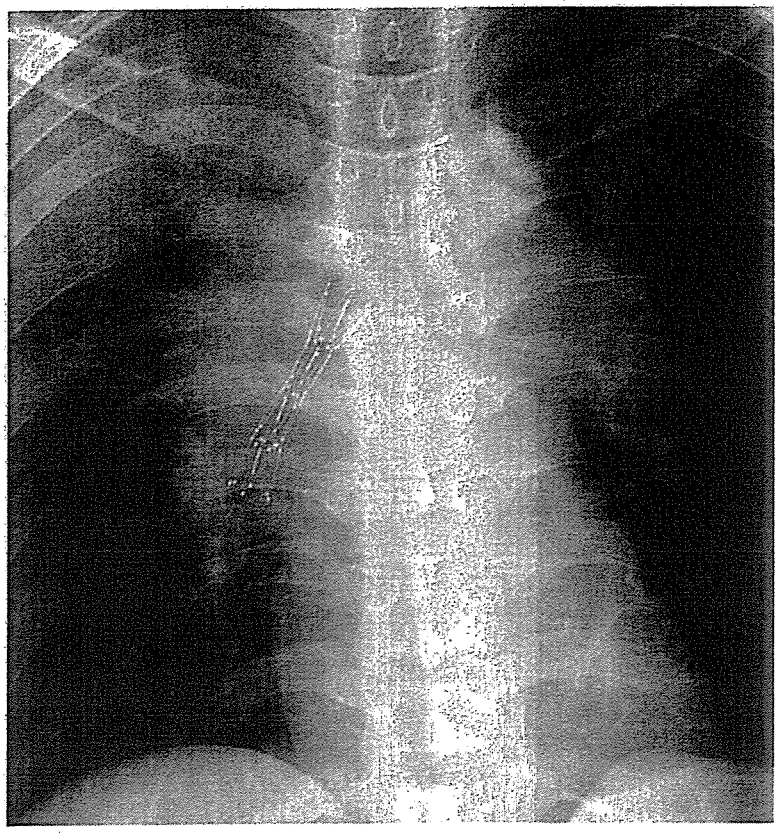

図2　右主気管支狭窄に対し挿入されたステント
ステントにより右主気管支の狭窄部は拡張し，十分な口径が確保されている．

不要となっている．

3）胆道の狭窄に対する治療

胆道の狭窄に対する治療は，現在最も多くメタリック・ステントが使用されている領域であり，PTCDルートを介して挿入する方法と内視鏡的に逆行性に挿入する方法とがある．メタリック・ステントは側枝を閉塞しないため，肝門部胆肝癌のような複数の胆管枝が狭窄している症例にも対応できる．398例を対象に行われた厚生省がん研究助成金（荒井班）による共同研究では，技術的成功率100%，重篤な合併症はなく，90%の症例で外瘻チューブが抜去されている．累積開存期間は6カ月74%，1年55%，2年32%であった．

4）消化管の狭窄に対する治療（図3）

消化管の狭窄は蠕動運動があるためメタリック・ステントが移動しやすく，また圧排による粘膜面のびらんや潰瘍形成，穿孔などの危険性があるため，他の領域に比べ合併症が問題となる頻度が高い．現在，最も汎用されているのは食道あるいは食道-胃・空腸吻合部の狭窄に対する治療であり，この他に直腸，左半結腸，十二指腸などが対象とされている．食道狭窄の場合にはcovered stentが用いられる場合が多い．183例を対象とした厚生省がん研究助成金（荒井班）による共同研究では，技術的成功率97%，臨床症状の改善が84%にみられている．反面，縦隔炎などの重篤な合併症がみられ，8%の症例の死因がメタリック・ステント留置と関連したものであった．消化管狭窄に対するメタリック・ステント留置はがん末期症例の経口摂取を可能にする点で有用である反面，重篤な合併症の危険性が少なくないため，施行にあたっては十分な検討と危険性についての情報開示を徹底する必要がある．

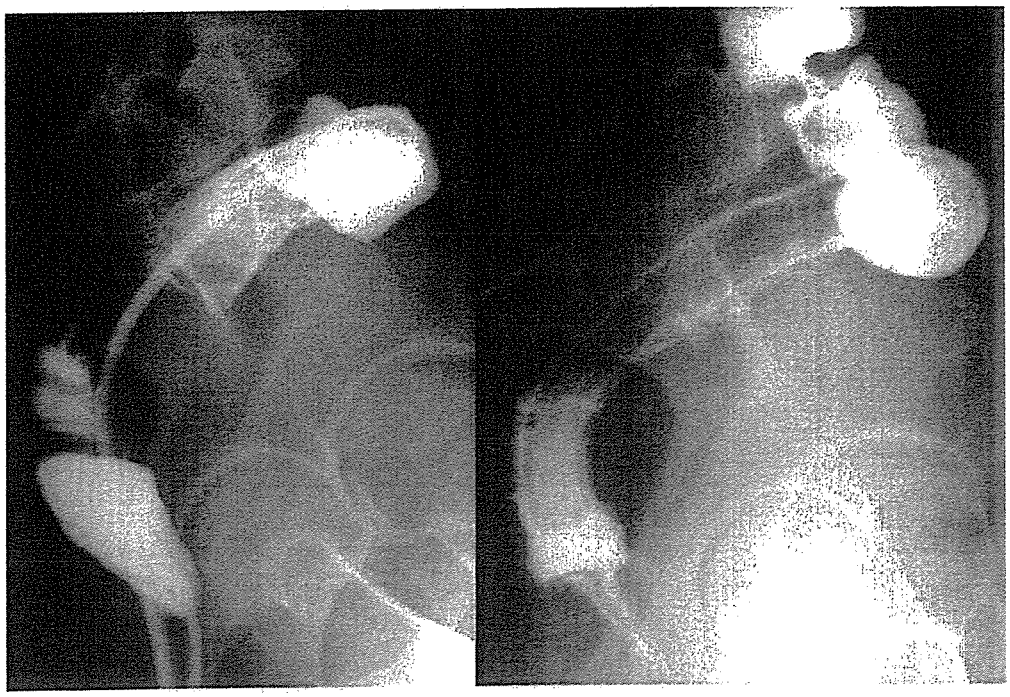

図3　腹膜播種による直腸狭窄に対し留置された直腸ステント

3. チューブ留置からの開放

病態の点で止むを得ないとはいえ，長期に留置されるチューブは患者のQOLを著しく低下させるものであり，これらのチューブの抜去を可能とすることも癌緩和医療におけるIVRの重要な役割のひとつである．経鼻チューブ，輸液や薬剤投与のための中心静脈カテーテル，ドレナージチューブなどがその対象となる．

1) 経皮経食道胃管挿入術（図4）

経腸栄養あるいは消化管閉塞に対するドレナージ目的で留置される経鼻チューブの苦痛を解除するために，頸部食道を直接穿刺し，ここからチューブを留置するものである．イレウスチューブを挿入することも可能であり，改善の見込みのない末期の癌性腹膜炎によるイレウス症例などがきわめてよい適応と言える．

2) 中心静脈カテーテルの埋め込み

治療のための血管確保としての観点から中心静脈カテーテルにポート（リザーバー）を接続して皮下に埋め込み，カテーテル管理の煩わしさや感染リスクを減らそうとするもので，すでに広く行われている．特に，在宅での輸液を継続する場合や持続的な抗癌剤投与を外来ベースで行う場合には必須の処置と言える．

3) ドレナージルートの内瘻化（図5）

胆管狭窄におけるメタリック・ステントによる内瘻化や尿管狭窄におけるW-Jカテーテルによる内瘻化など以外に遷延する膿瘍なども本来の流出下流側の狭窄が原因である場合には，メタリック・ステントによる内瘻化でチューブを抜去できる場合がある．

4) 骨転移による疼痛に対する治療（図6）

骨転移による疼痛や骨変形の進行を阻止する目的で，経皮的に骨転移巣へ針を刺入して骨セメントを注入する方法であり，下部胸椎，腰椎，骨盤骨などが対象となる．骨の強化による疼痛の軽減に加え，病的骨折を予防する点も期待されるが，放射線照射や化学療法など既存の抗癌治療との併用についての検討は未だなされていない．この他にラジオ波凝固を用いた骨転移の疼痛に対する治療も行われているが，未だ臨床試験の段階である．

図4　頸部食道から直接挿入された胃管

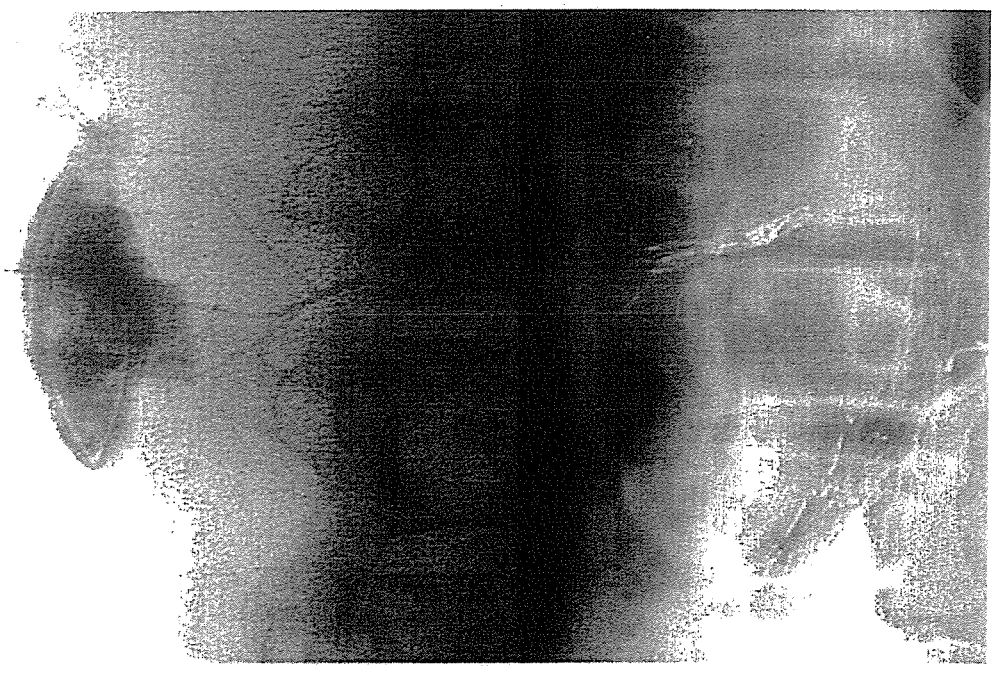

図5　遷延する肝膿瘍に対する内瘻化
当該部位の胆管狭窄をステントで拡張することにより，肝膿瘍は速やかに改善しチューブが抜去された．

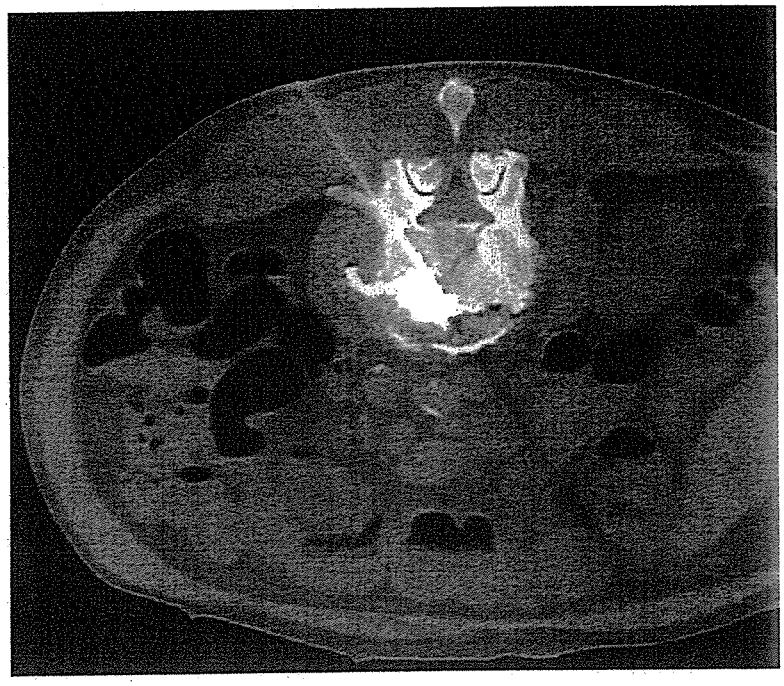

図6　椎体形成術
CTガイド下に椎体の骨転移部に針が刺入され，骨セメントが注入されている．

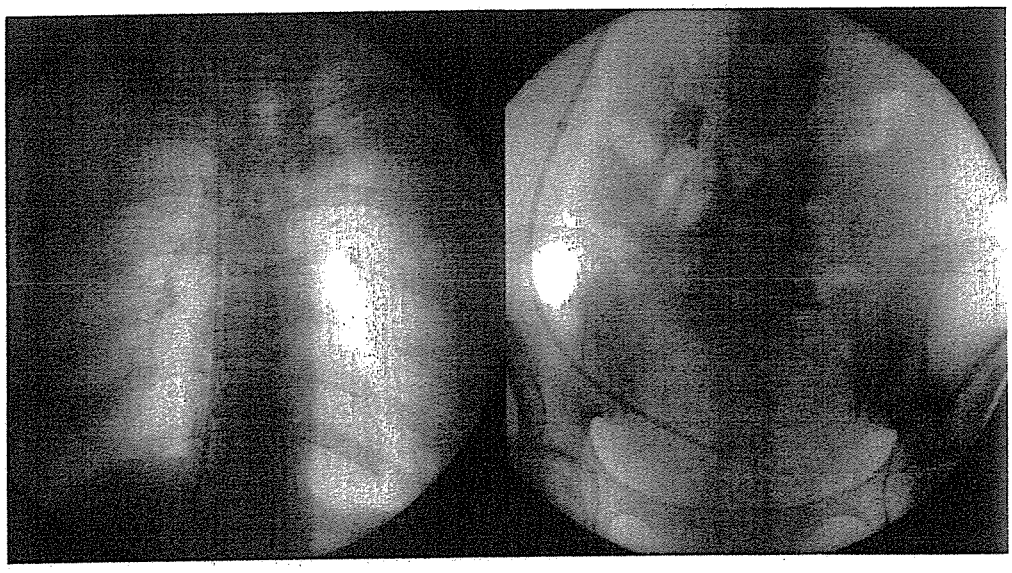

図7　経頸静脈経肝的腹水—静脈シャント
右頸静脈から挿入したカテーテルが，右肝静脈を通り，肝表面を穿破して骨盤腔に達して留置されている．腹水はカテーテル内部を上行し，逆流防止機能付側孔弁より右房に還流する．

4.　難治性腹水に対する治療（図7）

腹水を中心静脈に還流させるチューブを留置することにより，腹水を減少させるとともに，循環血漿量を増加させ全身状態の改善を図る方法である．従来からあるデンバーシャント（皮下トンネ

ルを介してシャントチューブを留置するもの）以外にも，肝静脈を介する血管経由で中心静脈と腹腔を結ぶ方法も開発されている．

5. IVR技術の応用

本来画像誘導なしでも可能な領域に画像誘導やIVR技術を導入することにより，手技に伴う侵襲を少なくし，またQOL向上を図ろうとするものである．例えば，通常ベッドサイドで盲目的に行われる鎖骨下静脈からの中心静脈カテーテルの挿入を，肘静脈から少量の造影剤を注入しながら透視下に行うことで安全性，確実性を高め，さらに手技に要する時間を短縮するなどが挙げられる．また，胸水や腹水のドレナージに際しても，セルジンガー法を用いることにより，より苦痛の少ない柔軟なチューブ留置することが可能であり，末期症例の胸水ドレナージのために大口径のトロッカー・カテーテルを留置するなどは到底許容し難い．このようにQOL向上のためにIVRが活用できる領域はきわめて広い．

6. IVRの問題点

IVRの問題点としては，以下の点が挙げられる．

①個々の症例の解剖や状況に即応しての器材と手技の選択が必要であるため手技の標準化が難しい，②術者の技量や使用する画像機器の性能が結果に大きく影響する，③臨床試験による評価が難しい，④新しい器材を使用する新しい治療であるため，しばしば規制当局の承認や保険対応等が間に合わず適正な医療報酬に繋がらない，⑤医療関係者における認知度が低く，十分に活用されていない．特に⑤の医療関係者における認知度が低い点は大きな問題であり，少なくとも緩和医療においては，その必須知識としてIVRが認知されるべきと思われる．ちなみに，わが国の臨床腫瘍学のテキストブックでは海外のものに比べ多くの頁がIVRに割かれている[7]．

7. IVRの臨床試験

IVRが十分に活用されるためには，臨床試験により明確なエビデンスが示され，IVRが癌緩和医療における標準的治療の一環に組み込まれる必要がある．IVRの臨床試験は，欧米も含め薬物療法などに比べ未だ大きく立ち遅れているのが，国内では海外に先行して厚生労働省がん研究助成金による研究班を母体に，2002年にがんのIVRについての臨床試験組織JIVROSG（Japan Interventional Oncology Study Group）が結成され，現在33組織が参加し，10の臨床試験が進められている（表1）[8]．また，欧米でもMedical Oncologistを交えInterventional OncologyとしてIVRを臨床試験により評価しようとする活動が本格化している．よって近い将来，臨床試験で示されたエビデンスに基づいてIVRが癌診療における標準的治療の一角として認知されることが期待される．

表1　JIVROSGにおける臨床試験

Phase Ⅰ/Ⅱ
経頸静脈経肝的腹水—静脈シャント造設術（進行中）
経皮的椎体形成術（進行中）
肺腫瘍に対するラジオ波凝固療法（進行中）
骨腫瘍に対するラジオ波凝固療法（進行中）
骨盤内腫瘍に対するラジオ波凝固療法（進行中）
肝内胆管がんに対する塩酸ゲムシタビン肝動注療法（進行中）
子宮筋腫に対するゼラチンスポンジによる動脈塞栓療法（進行中）
肝細胞がんに対するシスプラチン＋ゼラチンスポンジによる動脈塞栓療法（計画中）
Phase Ⅱ
経皮経食道胃管挿入術（進行中）
大腸狭窄に対するステント治療（進行中）
大静脈狭窄に対するステント治療（計画中）
Phase Ⅲ
胆道狭窄に対するベア・ステントとカバード・ステントの比較試験（進行中）

まとめ

癌緩和医療に関わるIVRを紹介した．IVRは癌緩和医療においてきわめて有用な治療手段であるが，このIVRが活用されるか否かは，緩和医療に携わる医療従事者が眼前の患者を診たときにIVRを思いつくか否かにかかっている．いまや癌緩和医療における必須の治療手段として，常にIVRを思い起こしていただくことに本稿が役立

てば幸いである.

文　献

1) Margulis AR: Interventional Diagnostic radiology-A subspeciality. *Am J Roentgenol* **99**: 761–762, 1967
2) Wallace S: Interventional radiology. *Cancer* **37**: 517–531, 1976
3) 荒井保明：6–30 Interventional Radiologyの手技を用いた治療法の有効性に関する研究．厚生省がん研究助成金による研究報告集　平成6年度，国立がんセンター，東京，459–463, 1994
4) 荒井保明：6–30 Interventional Radiologyの手技を用いた治療法の有効性に関する研究．厚生省がん研究助成金による研究報告集　平成7年度，国立がんセンター，東京，242–247, 1995
5) 荒井保明：8–26 Interventional radiologyの手技を用いた治療法の有効性についての研究．厚生省がん研究助成金による研究報告書　平成8年度，国立がんセンター，東京，422–426, 1996
6) 荒井保明：8–26 Interventional radiologyの手技を用いた治療法の有効性についての研究．厚生省がん研究助成金による研究報告書　平成9年度，国立がんセンター，東京，1996
7) 臨床腫瘍学（日本臨床腫瘍学会編），癌と化学療法社，東京，2003
8) 荒井保明：14–5 がん治療におけるIVRの技術向上と標準化に関する研究．厚生労働省がん研究所助成金による報告書　平成15年度，国立がんセンター，東京，2003

Consistent Liver Metastases in a Rat Model by Portal Injection of Microencapsulated Cancer Cells

Tsuyoshi Enomoto,[1] Tatsuya Oda,[1] Yasuyuki Aoyagi,[1] Shinji Sugiura,[3] Mitsutoshi Nakajima,[4] Mitsuo Satake,[5] Masayuki Noguchi,[2] and Nobuhiro Ohkohchi[1]

Departments of [1]Surgery (Graduated School of Comprehensive Human Science) and [2]Pathology, Institute of Basic Medicine, University of Tsukuba; [3]Research Center of Advanced Bionics, National Institute of Advanced Industrial Science and Technology; [4]Food Engineering Division, National Food Research Institute, Tsukuba, Ibaraki, Japan; and [5]Radiology Division, National Cancer Center Hospital East, Kashiwa, Chiba, Japan

Abstract

Consistent liver metastases in animal models is generally observed only with certain cancer cell lines. With the aim of improving on existing animal models of liver metastases, we hypothesized that cancer cells encased in 300 μm microcapsules, mimicking micrometastatic foci, might be effective seeds of liver metastases. A total of 3,000 microcapsules, containing 700 to 1,500 viable cells/capsule in logarithmic growth phase of three human pancreatic cancer cell lines (SUIT-2, AsPC-1, and BxPC-3), were transplanted in nude rats by portal injection. The rate of liver metastases was 100% (12 of 12), 100% (6 of 6), and 83% (5 of 6) for SUIT-2, AsPC-1, and BxPC-3 microcapsules, respectively. In contrast, the administration of an identical number of single cancer cells (2.1–4.5 × 10^6) did not lead to liver metastases. Metastases was strictly limited to the liver, was quite stable, and could be proportionately tailored by varying the number of cancer microcapsules administered. Microscopic observation showed that two-thirds of the cancer microcapsules were lodged in the peripheral small (20–50 μm) portal veins, although one-third of the cancer microcapsules were trapped in the central wide (200–400 μm) portal vein. Capsules began to burst at day 3, with recognizable metastases produced at day 7, resulting in overt metastases production at days 28 to 42. The present cancer microcapsule method may be useful for obtaining liver metastases in animal models, especially for cell lines that will not form liver metastases with conventional single cell injection methods and/or for experiments requiring the consistent formation of liver metastases. (Cancer Res 2006; 66(23): 11131-9)

Introduction

Liver metastases is one of the most common forms of hematogenous spread in patients with various malignancies (1, 2), and the development of effective treatment modalities for liver metastases using convenient animal models is highly desirable. Because the liver is the largest solid organ, a reliable animal model of liver tumors is also valuable for *in vivo* evaluation of various therapeutic agents. However, representation of liver metastasis in an animal model using conventional approaches has proved difficult.

One commonly used approach for obtaining liver metastases is by injecting cancer cell suspensions into the hepatic portal veins or the spleen (3). However, liver metastases are consistently generated only with certain cell lines of the pancreas, colon, and stomach that have a high metastatic potential to liver (4–8). Moreover, many cell lines do not generate consistent liver metastases when administered as single cell suspensions (7–9). An additional obstacle with this model is that tumor growth occurs in sites other than the liver, such as the injected spleen and/or peritoneum (10). In fact, these undesirable tumor growths make experiments focusing on liver metastases difficult to interpret and largely inhibit the appearance of liver metastases (11, 12). Alternative strategies for obtaining liver metastases with cancer cells of low metastatic potential include orthotopic implantation, by injecting cancer cell suspensions, or by surgical transplantation of tumor fragments (13–15). Obstacles in the latter strategy include the presence of undesired metastases and are moreover difficult to reproduce in terms of the frequency and extent of metastases (16–18).

The formation of hematogenous metastases has been explained by two major theories, i.e., the seed and soil hypothesis by Paget (19) and the anatomic mechanical trapping theory of Ewing (20). The former suggests that metastases occurs only when the metastatic capacity of certain cancer cells (= seed) and environments of target organs (= soil) are compatible. The latter theory proposes that the anatomic location of the primary tumor and target organs, i.e., nonspecific trapping of cancer cells in the microvasculature, plays an important role in the development of metastases. Both mechanisms may also jointly contribute to the development of liver metastases in a clinical setting. The fact that even pancreatic cancer cell lines, which are clinically notorious for frequent presentation of liver metastases, do not consistently present liver metastases in animals (7, 8) forces the consideration that one of the difficulties in developing liver metastases in an animal model may be that the mechanical trapping process is not adequately reproduced.

With the aim of improving on existing animal models of liver metastases, we hypothesized that mechanical trapping could be rendered more efficient by aggregating multiple cancer cells. For this purpose, we employed cell encapsulation technology, previously used for pancreatic islet cell transplantation (21), which enabled us to consistently encase cancer cells into uniform 300 to 700 μm capsules. The preincubation of cancer cell containing cancer microcapsules *ex vivo* could substitute the initial proliferation step of cells, effectively providing cells in the logarithmic growth phase. When these cancer microcapsules are injected in the portal vein, they may become physically trapped in the peripheral vasculature of the liver before bursting and could thus act as seeds of liver metastases.

Note: Y. Aoyagi is a recipient of a Postdoctoral Fellowship from the Japan Society for the Promotion of Science, Tokyo, Japan.

Requests for reprints: Tatsuya Oda, Department of Surgery, Institute of Clinical Medicine, University of Tsukuba, 1-1-1 Tennondai, Tsukuba, Ibaraki 305-8575, Japan. Phone: 81-298-53-3221; Fax: 81-298-53-3222; E-mail: tatoda@md.tsukuba.ac.jp.

doi:10.1158/0008-5472.CAN-06-0339